Mössbauer-effect and x-ray-absorption spectral study of sonochemically prepared amorphous iron

Gary J. Long and Dimitri Hautot
Department of Chemistry, University of Missouri-Rolla, Rolla, Missouri 65409-0010

Quentin A. Pankhurst
Department of Physics and Astronomy, University College London, London WC1E 6BT, United Kingdom

D. Vandormael, F. Grandjean, and J. P. Gaspard
Institut de Physique, B5, Université de Liège, B-4000 Sart-Tilman, Belgium

Valérie Briois
Laboratoire pour l'Utilisation du Rayonnement Electromagnétique, Université de Paris Sud, F-91405 Orsay, France

Taeghwan Hyeon and Kenneth S. Suslick
School of Chemical Sciences, University of Illinois at Urbana-Champaign, Urbana, Illinois 61801
(Received 10 November 1997)

The Mössbauer spectra of amorphous iron, prepared by using sonochemical methods, exhibit a broad magnetic hyperfine sextet at both 78 and 295 K. The spectra do not change with time if the amorphous iron is not exposed to oxygen or moisture. An analysis of the spectra with the method of Lines and Eibschütz yields average magnetic hyperfine fields of 29.1 and 25.9 T at 78 and 295 K, respectively. The corresponding moments of $1.9\mu_B$ and $1.7\mu_B$ agree well with values obtained from earlier magnetization studies and, further, provide strong experimental support for earlier calculations of the magnetic moments in amorphous iron. The observed average isomer shifts of 0.27 and 0.14 mm/s obtained at 78 and 295 K, respectively, correspond to a decrease in the *s*-electron density at the iron-57 nucleus as compared to that of α-iron, a decrease which is consistent with the decreased coordination number of amorphous iron. The similarity of the 295 K iron *K*-edge x-ray-absorption spectrum of amorphous iron and α-iron, up to 7130 eV, indicates that the *d*-electron density of states just above the Fermi level is similar in both forms of iron. The absence of structural details above 7130 eV in the spectrum of amorphous iron indicates, in agreement with multiple-scattering calculations, that long-range order does not extend beyond the third shell of neighbors in amorphous iron. Greatly reduced extended x-ray-absorption–fine-structure scattering is observed at the iron *K* edge of amorphous iron as compared to α-iron. An analysis of the weak observed scattering reveals both a decrease in the average coordination number from 14 in α-iron to 10 in amorphous iron, and an asymmetric radial distribution function of the iron neighbors in the first shell. This asymmetric distribution yields for amorphous iron a minimum iron-iron distance of 2.40 Å and an average iron-iron distance of 2.92 Å. [S0163-1829(98)08817-1]

I. INTRODUCTION

Amorphous metallic alloys are often obtained by the rapid quenching of their melt and, as a consequence, they lack any long- or short-range atomic order. This metallic glassy state is rather different than that typically found in conventional glasses that often contain large molecular anions or long covalently bonded chains that help to stabilize the glassy state. Thus to stabilize amorphous metallic alloys, glass formers, such as boron, carbon, or phosphorus, are often added to the melt. Hence, the resulting glassy material is not a pure elemental amorphous material, as is the material studied in this paper.

Because elementally pure amorphous materials are disordered locally, but not chemically, they can very easily crystallize, and it has been predicted[1] that amorphous iron can only be obtained with very rapid quenching rates of the order of 10^9 deg/s or faster. Unfortunately, these extremely rapid quenching rates cannot be obtained by conventional methods and for many years it was accepted that amorphous iron did not exist, at least at temperatures near room temperature. In contrast, amorphous iron and cobalt can be prepared[2] at 20 K as thin films, films that subsequently have to be kept at 20 K to maintain the amorphous state.

Suslick and his co-workers[3–6] have shown that sonochemical techniques can lead to quench rates greater than 10^9 deg/s in sonochemically generated bubbles that can have internal temperatures as high as 5000 K. More recent calculations[7] have indicated that the actual temperatures may be as much as two orders of magnitude higher. By using this technique Suslick and his co-workers have been able to prepare essentially pure amorphous iron[8] and have reported on its structural and magnetic properties.[9–11] Other laboratories have reported on the sonochemical preparation of amorphous nickel,[12] amorphous iron-nickel alloys,[13] on the coating of

amorphous iron,[14] and on the control of the particle size of amorphous iron.[15]

Because of the potential technological importance of amorphous elemental iron,[16] we have undertaken a Mössbauer and x-ray-absorption spectral study of the structural and magnetic properties of amorphous iron.

II. EXPERIMENT

A sample of amorphous elemental iron was prepared sonochemically from $Fe(CO)_5$ by the previously reported method.[8] The resulting shiny black powder was found by chemical analysis to contain, by weight, $(100\pm0.5)\%$ iron, $(1.6\pm0.2)\%$ carbon, $(0.1\pm0.2)\%$ hydrogen, $(0.0\pm0.2)\%$ oxygen, and $(0.0\pm0.2)\%$ nitrogen, and thus this sample contains much less carbon than the sample reported upon earlier.[8,10,11] It should be noted that, in terms of atomic percent, the new sample corresponds to $Fe_{93}C_7$ or $Fe_{88}C_7H_5$. However, an x-ray powder-diffraction pattern of the sample revealed, as in the earlier case,[8] no trace of any crystalline material, including α-iron. Also, heating above the glass crystallization temperature[8] led to the observation of only α-iron in the resulting powder x-ray-diffraction pattern. Thus we believe the carbon is associated with surface contamination and that it is reasonable to refer to the material as pure elemental amorphous iron. As expected, the sample was extremely moisture and air sensitive and all subsequent manipulations of the sample were carried out under an inert atmosphere.

The Mössbauer spectra were measured at 78 and 295 K on conventional constant-acceleration spectrometers which utilized a room-temperature rhodium-matrix cobalt-57 source and were calibrated at room temperature with α-iron foil. The studies were limited to these temperatures because of the requirement that the amorphous iron could not be exposed to oxygen or moisture and because of the limitations of our experimental facilities. The absorber, which was prepared in a Vacuum Atmospheres, Inc. inert-atmosphere dry box under pure nitrogen, contained 26 mg/cm^2 of material finely dispersed in deoxygenated Vaseline. The absorber was then placed in a cryostat that could be sealed in the dry box and subsequently studied in the Mössbauer spectrometer at the University of Missouri-Rolla. In this way we could obtain the spectra on a sample that had never been exposed to oxygen or moisture. Because amorphous iron could be unstable with time, we have remeasured the spectra of the same absorber again, after six months, at the University of Missouri-Rolla and then again, after approximately one year, at University College, London. In each instance, virtually identical spectra were observed, indicating no change with time for the material, at least over a year while maintained sealed at room temperature under an inert atmosphere.

The x-ray-absorption spectra were recorded with the synchrotron radiation provided by the DCI storage ring at the Laboratoire pour l'Utilisation du Rayonnement Electromagnétique, Université de Paris Sud, France. The synchrotron radiation was produced by a storage ring operated with 1.85 GeV positrons and with a maximum beam intensity of ca. 300 mA. The measurements were performed with the EXAFS III spectrometer that uses a double crystal silicon (311) monochromator and were carried out in the transmission mode with ionization chambers in front and behind the absorber. A pellet of the compound, with an area of 1 cm^2 and a mass of ca. 30 mg, was pressed and maintained in an inert atmosphere. The extended x-ray-absorption–fine-structure (EXAFS) spectra were recorded at 295 K with a 2 eV step and with a one-second accumulation time per step over a 1000 eV energy range. The x-ray-absorption–near-edge structure (XANES) spectra were recorded with a 0.25 eV step over a 125 eV energy range. The spectrum of a standard iron foil was recorded before and after the measurements in order to calibrate the energy. The first derivative of the iron-foil K-edge spectrum at 7112 eV was used to define the zero-energy reference point of the resulting spectra.

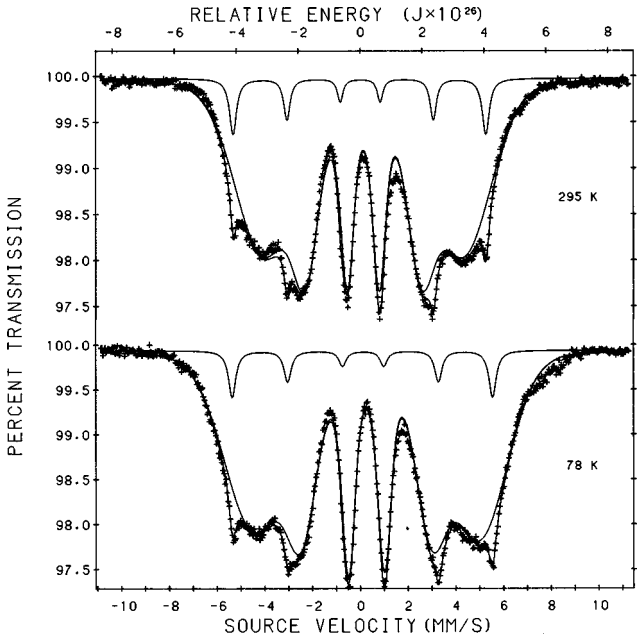

FIG. 1. The Mössbauer spectra of amorphous iron obtained at 295 and 78 K. The solid lines correspond to a fit obtained using a Lines and Eibschütz Voigtian line profile analysis, see text.

III. RESULTS AND DISCUSSION

A. Mössbauer spectra

The Mössbauer spectra of amorphous iron, obtained at 78 and 295 K, are shown in Fig. 1. It is immediately obvious from this figure that the spectra consist of two components, a broad sextet, typical of an amorphous material, and a relatively sharp sextet that seems typical of crystalline α-iron. Because of the presence of these two components, we have chosen to analyze the spectra in terms of a Lines and Eibschütz-type[17] Voigtian profile of Lorentzian components for the sextet with the distribution of hyperfine parameters observed for the amorphous-iron component, and one Lorentzian sextet, with parameters virtually the same as those of α-iron, for the sharp component. In all cases the linewidth of the Lorentzian components was constrained to be 0.24 mm/s, a value that is appropriate for the experimental linewidth observed in both spectrometers used in the experiments. Further, the relative areas of each of the six lines in each sextet were constrained to be in the ratio of $3{:}x{:}1{:}1{:}x{:}3$. The resulting parameters, averaged over all the measured spectra, are presented in Table I, along with the

TABLE I. Mössbauer spectral hyperfine parameters. The average of three separate measurements in two different laboratories at 295 K and two separate measurements in the same laboratory at 78 K on the same absorber. The numbers in parentheses represent the error in the values as determined by the analysis of the spectra as discussed in the text.

Component	Parameter	295 K	78 K
Amorphous iron	$\langle H\rangle$, (T)	25.9(3)	29.1(3)
	$\langle\mu\rangle$ (μ_B)	1.7(1)	1.9(1)
	$\langle\Delta H\rangle_{\rm rms}$ (T)[a]	10.5(10)	12.4(1.2)
	$\langle\delta\rangle$ (mm/s)[b]	0.14(1)	0.27(1)
	$\langle\Delta\delta\Delta H\rangle$ [(mm/s)^2][c]	0.29(4)	0.09(3)
	x	1.37(2)	1.48(2)
	% area	94(1)	95(1)
	Abs. area [(%ε)(mm/s)]	16.45(5)	19.52(5)
	$d\delta/dT$ [(mm/s)/K]	$-6.0(4)\times10^{-4}$	···
	$M_{\rm eff}$ (g/mol)	70(5)	···
	$d(\ln A)/dT$ (K^{-1})	$-7.89(5)\times10^{-4}$	···
	θ_M (K)	377(5)	···
α-iron	H (T)	32.9(3)	33.9(4)
	δ (mm/s)	0.00[d]	0.10
	% area	6(1)	5(1)

[a]The root-mean-square deviation of the hyperfine field relative to ΔH.

[b]The isomer shifts are reported relative to room-temperature α-iron foil.

[c]The isomer shift and hyperfine-field fluctuation correlation.

[d]Parameter constrained to value given.

estimated error, as determined from the Lines and Eibschütz analysis. These fits are represented by the solid lines in Fig. 1. At this point it is not clear why x increases slightly upon cooling, but the observed values clearly indicate the presence of some magnetic texture in the absorber. As expected, no quadrupole interaction was apparent at either temperature.

The spectral component attributed to amorphous iron in Fig. 1 very much resembles that observed[17–22] for $Fe_{80}B_{20}$ and related glassy metalloid materials. The corresponding mean magnetic moment $\langle\mu\rangle$ obtained from the mean hyperfine field with the generally accepted proportionality constant of 15 T/μ_B, is given in Table I. The $1.7\mu_B$ moment obtained from the 295 K Mössbauer spectrum of amorphous iron agrees perfectly with the moment derived earlier[10] from the Bloch-law temperature dependence of the magnetization of amorphous iron. Further, both of these observed moments provide experimental support for the recent *ab initio* linear muffin-tin atomic-sphere approximation calculations of Liebs and Fähnle,[23] calculations that yielded a 295 K moment of $(1.8\pm0.4)\mu_B$ for a statistically disordered array of spins.

The observed 295 K isomer shift of amorphous iron is, as expected, larger than that of α-iron as a consequence of a decrease in the average coordination number. It should be noted that α-iron, with a density of 8.9 g/cm^3, has a coordination shell of 14 atoms at an average distance of 2.65 Å, involving eight atoms at 2.48 Å and six atoms at 2.87 Å. This corresponds to a density of 0.180 iron atoms/Å^3. A mean-field analysis[10] of the Bloch-law temperature dependence of the magnetization of amorphous iron yielded an average of ca. 10 near neighbors, a value in agreement with the 10 ± 1 value found in an extended x-ray-absorption–fine-structure study[2] of an amorphous iron thin film at 20 K. As discussed below, an EXAFS study of amorphous iron, which has a reported[9] density of 6.03 g/cm^3, yields a coordination shell of 10 atoms at an average distance of 2.92 Å. This corresponds to a density of 0.096 iron atoms/Å^3. Hence, the decreased number of iron atoms per unit volume in amorphous iron increases the radial expansion of the iron $4s$ valence electrons, and thus the isomer shift, as compared to α-iron.

The temperature dependence of the isomer shift of amorphous iron, although admittedly based on only two data points, yields[24] an effective recoil mass $M_{\rm eff}$ of 70 g/mol, a value that is larger than the value of 65 g/mol observed[25] for α-iron. This increase in effective recoil mass results from the decreased number of near neighbors and the corresponding increase in the covalency of the bonding in amorphous iron as compared to α-iron. The temperature dependence of the isomer shift and the absolute spectral absorption area yield[24] the effective Mössbauer temperature, θ_M, a quantity that is similar to the Debye temperature. The observed value of 377 K is somewhat larger than the value of 345 K observed[26,27] for nanostructured iron but is, as expected, substantially lower than the value of ca. 467 K reported for α-iron.[26]

The presence of ca. 5% of a component closely resembling α-iron in the spectra of amorphous iron calls for special comment. Because the percentage area of this component neither increases nor decreases with time, we do not believe that it results from the crystallization with time of the amorphous iron, but rather we believe that this sextet is intrinsic to the originally prepared material, and is probably due to very fine form ferromagnetic particles of 1–5 nm in diameter. Indeed, Mössbauer spectra[26] of nanostructured iron particles with a 1–10 nm diameter consist of two sextets, one typical of α-iron and one assigned to iron at the boundary of the particles. Hence, the α-iron-like component observed

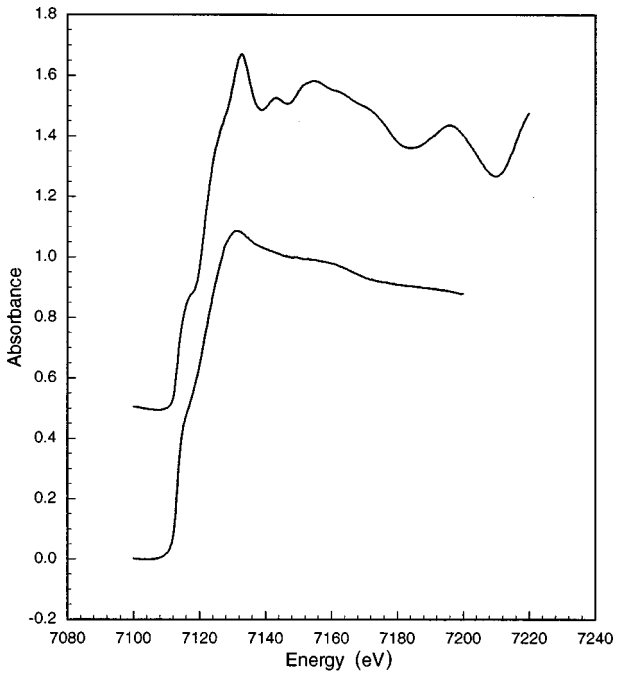

FIG. 2. The iron K-edge x-ray-absorption spectra of α-iron, upper curve, and amorphous iron, lower curve, measured at 295 K.

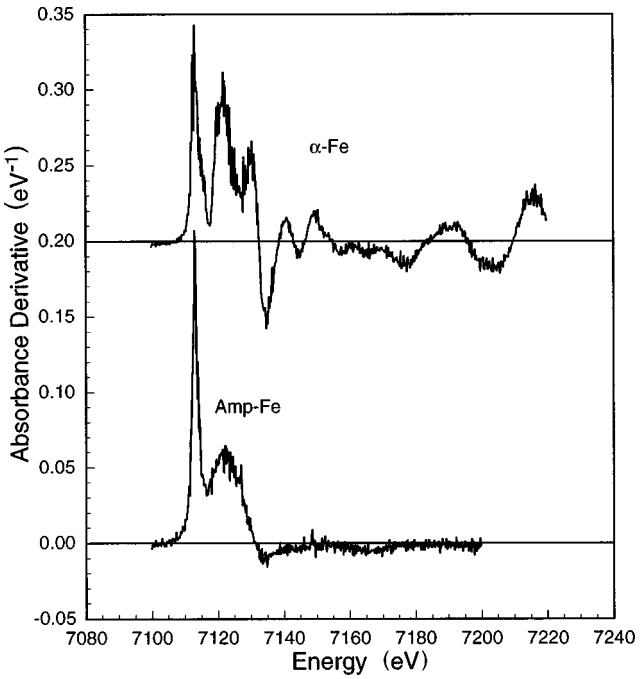

FIG. 3. The first derivative of the iron K-edge x-ray-absorption spectra of α-iron, upper curve, and amorphous iron, lower curve, measured at 295 K.

herein is quite compatible with the presence of particles of 1–5 nm diameter. Transmission-electron micrographs[5,8] of different amorphous iron samples revealed ca. 20 nm aggregate particles consisting of smaller 4–6 nm particles and show no crystallites larger than 4 nm. We have simulated x-ray-diffraction patterns for a mixture of 95% of 1-nm-diam particles representing the amorphous iron and 5% of 4, 8, and 16 nm-diam particles representing the crystalline α-iron. These simulations revealed that the crystalline component is easily distinguishable for diameters of 8 and 16 nm, and is not distinguishable for a diameter of 4 nm or less, in perfect agreement with the particle size observed by electron microscopy. However, it is not possible from the Mössbauer spectra to show definitively that the component is α-iron. Indeed, unpublished spectra,[28] obtained with a source consisting of cobalt-57 annealed into an α-iron matrix, do reveal small differences in this component as compared to the known spectrum of α-iron obtained with such a source.

B. X-ray-absorption spectra

The iron K-edge x-ray-absorption spectra of α-iron and amorphous iron, measured at 295 K, are shown in Fig. 2 and the first derivative of these spectra are shown in Fig. 3. The spectrum of α-iron is essentially the same as that reported previously.[29,30] In contrast, and as expected, the spectrum of amorphous iron reveals much less detail. However, as shown by a minimum in the first derivative of the spectra, see Fig. 3, both α-iron and amorphous iron show a distinct shoulder, see Fig. 2, at 7117 eV, i.e., at 5 eV above the Fermi level of α-iron, which is 7112 eV, the energy of the maximum in the first derivative of the K-edge spectrum of α-iron. As shown in Fig. 2, the maximum in the spectral absorbance occurs at 7133 and 7131 eV, i.e., at 21 and 19 eV above the Fermi level, in α-iron and amorphous iron, respectively.

The α-iron K-edge x-ray-absorption spectra have been calculated using the linearized augmented-plane-wave method[31] and the results indicate that the peaks up to ca. 30 eV in energy above the Fermi level are associated with transitions of the 1s electron to partially filled bands with a large d-electron density of states hybridized with the p electron. The calculated spectrum[31] has a very close resemblance to the initial absorptions observed for both α-iron, and amorphous iron, see Fig. 2. Indeed, the calculated spectrum shows a ca. 15 eV splitting between the initial shoulder and the maximum in absorbance, a splitting that agrees well with the 16 and 14 eV splittings observed herein for α-iron and amorphous iron, respectively. Thus it would appear that the d electron hybridized with the p-electron density of states just above the Fermi level is quite similar in both α-iron and amorphous iron.

The structure observed above the maximum in absorbance in the spectra of both α-iron and amorphous iron, i.e., above ca. 7130 eV, results from multiple-scattering processes.[30,31] As is clearly indicated in both Figs. 2 and 3, above this maximum in absorbance the scattering by amorphous iron shows much less structure than that of α-iron. This difference is also obvious in Fig. 4 that shows the EXAFS scattering observed for both amorphous iron and α-iron. We have carried out multiple-scattering calculations on α-iron for clusters of 15, 27, and 89 iron atoms, corresponding to two, three, and seven shells of iron atoms, respectively. These calculations show that the peak at ca. 7140 eV in the spectrum of α-iron in Fig. 2 is not present with three shells but is present with seven shells of iron atoms. Because this peak disappears in the spectrum of amorphous iron in Fig. 2, we can conclude that the long-range order in the amorphous iron does not extend beyond three or at most four shells of iron atoms, i.e., within a sphere of 4–5 Å radius.

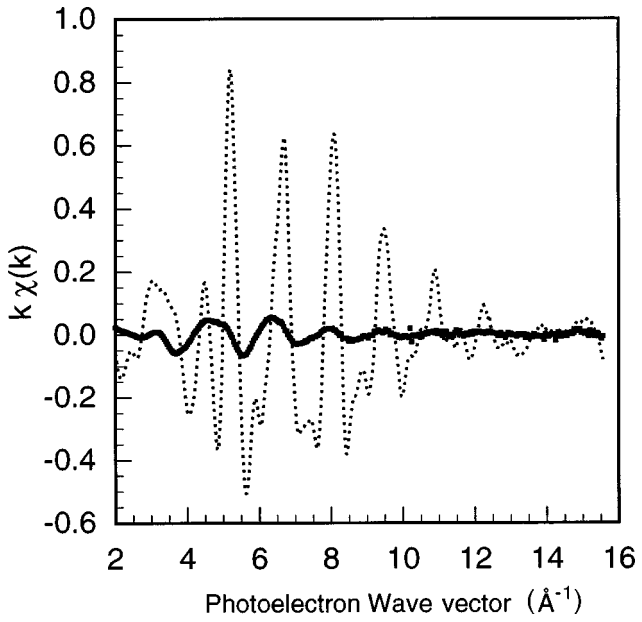

FIG. 4. The iron *K*-edge extended x-ray-absorption fine structure of α-iron, dotted line, and amorphous iron, solid line, measured at 295 K.

C. EXAFS spectra

The scattering observed in the extended x-ray-absorption–fine-structure study of amorphous iron, see Fig. 4, is much less than that observed in α-iron and that observed earlier[2] for an amorphous iron thin film. However, when the amorphous iron thin film[2] was annealed at 300 K the resulting scattering was virtually identical to that which we obtained for α-iron, see Fig. 4. As expected, the results for α-iron are also virtually identical to those reported earlier.[29–33]

The Fourier transforms of the extended x-ray-absorption–fine-structure results for amorphous and α-iron are shown in Fig. 5. The transform for α-iron is identical to those published earlier.[2,31,32] In α-iron the first two-shell peak has been filtered in the range of 1.4–3.0 Å, inverse Fourier transformed, and analyzed with eight iron neighbors at 2.48 Å and six iron neighbors at 2.87 Å, in agreement[33] with the known bcc structure of α-iron. For our purposes, we will consider that the first coordination shell consists of these 14 iron atoms at two different distances, in the ratio of $2/\sqrt{3} = 1.16$, with a weighted average distance of 2.65 Å.

From a comparison of the positions of the first two peaks in Fig. 5, one can immediately conclude that the first coordination shell in amorphous iron is at a shorter distance than in α-iron. A similar conclusion was reached by Harris *et al.*[34] who studied by EXAFS amorphous $Fe_{80}B_{20}$ thin films. Hence, we expect a coordination number in amorphous iron that is smaller than 14, that of α-iron. The first shell peak in the Fourier transform for amorphous iron has been filtered, inverse Fourier transformed, and analyzed as explained below.

The 295 K filtered and back-Fourier-transformed EXAFS spectrum of amorphous iron, its Fourier transform, and their fits are shown in Figs. 6(a) and 6(b). It has been shown[35] that fits of the EXAFS spectra of highly disordered compounds with a symmetric Gaussian radial distribution function led to

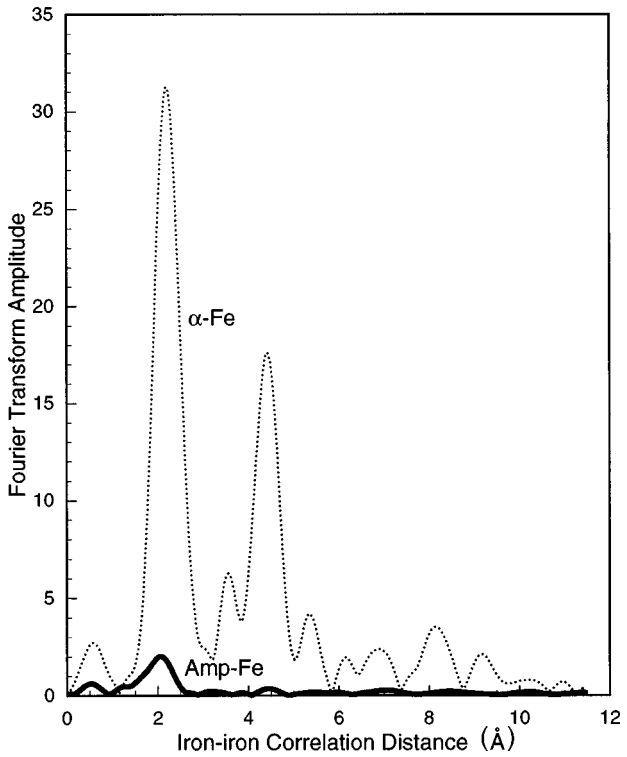

FIG. 5. The Fourier transform of the iron *K*-edge extended x-ray-absorption fine structure of α-iron, dotted line, and amorphous iron, solid line.

errors in distances and the number of neighbors. Our attempts to fit the EXAFS spectrum of amorphous iron with a symmetric Gaussian radial distribution function confirm these difficulties. To overcome them, the cumulant expansion has been used[2] to fit the amorphous-iron thin film with the assumption that hcp cobalt could be used as a reference. This expansion was not used herein because no reference hcp cobalt data were available. Thus, we have used an asymmetric hard-sphere-like radial distribution function[35] given by

$$P(r) = \frac{N}{2s}\exp[-(r-R)/s] \times \exp(\sigma^2/2s^2)\{1+\mathrm{erf}[(r-R)/\sqrt{2}\sigma]\},$$

$$\mathrm{erf}(z) = \frac{2}{\sqrt{\pi}}\int_0^z e^{-t^2}dt$$

The parameters of the fit for amorphous iron with such an asymmetric distribution are given in Table II. The asymmetric distribution is characterized by two parameters, σ and s, where σ corresponds to the usual Debye-Waller factor and s represents the width of the distribution due to the statistical disorder in the neighboring distances. The σ value of 0.083 Å compares well with the weighted average value of 0.079 Å found for the first shell in the reference α-iron. The R value of 2.40 Å given in Table II is the minimum distance between two iron atoms. This value compares well with the iron covalent radius of 1.17 Å and the iron-twelve-coordinate metallic radius of 1.26 Å. The average iron-iron distance in the asymmetric distribution is given by $R+s$ and is 2.92 Å, a value which is larger than the average value of 2.65 Å ob-

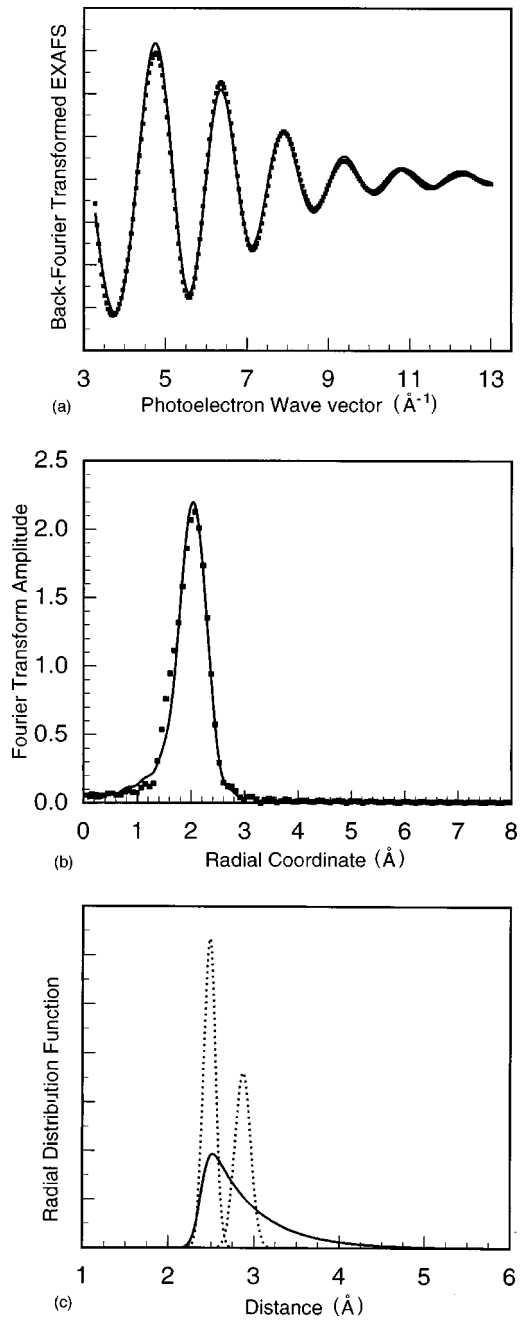

FIG. 6. The 295 K amorphous iron back-Fourier transformed EXAFS spectrum (a) and the Fourier transform (b) at the iron K edge. The solid lines represent a fit with the model described in the text and in Table II. The radial distribution functions of the first shell for amorphous iron, solid line, and α-iron, dotted line, are shown in (c). In this plot the areas under the distributions have been normalized to 10 for amorphous iron and 14 for α-iron.

served in α-iron and larger than the values of 2.56 and 2.64 Å found by neutron diffraction[9,11] and of 2.55 Å measured at 20 K on the 20 Å amorphous-iron thin films. The value of ten iron near neighbors is similar to that obtained[2] from EXAFS measurements on a 20 Å amorphous-iron film, but is larger than the value of 8.7 found[11] by neutron diffraction on amorphous iron. Further, because a density of 6.03 g/cm^3 was measured[9] by neutron-diffraction measurements for amorphous iron, we calculate that the filling of the space around an iron atom should be ca. 75% of that in α-iron. The ten iron near neighbors in amorphous iron, as compared to 14 in α-iron, correspond to a ca. 71% filling of the space around a specific iron atom.

TABLE II. EXAFS spectral analysis for amorphous iron at 295 K. The estimated errors are given in parentheses.

Neighbor	N	R (Å)	σ (Å)	s (Å)
Iron	10.00(1)	2.40(1)	0.083(1)	0.52(1)
Oxygen	2.18(5)	1.99(2)	0.23(2)	0.00[a]

[a]This parameter was not varied.

The radial distribution function, calculated[35] from the parameters given in Table II, is shown in Fig. 6(c), along with the radial distribution function for the first shell of α-iron. The shape of this function agrees very well with the conclusions drawn by Chandesris *et al.*[2] about the radial distribution functions in thin films of amorphous cobalt and iron. Specifically, the function has a steep edge at short distances and a long tail at large distances and the width of the function at half maximum is larger than that of the two Gaussian peaks for α-iron. Further, the function in Fig. 6(c) has its maximum at a distance of 2.525 Å, a value that agrees very well with the ca. 2.53 value observed[2] in the amorphous iron thin film. A visual comparison of the amorphous iron radial distribution function shown in Fig. 6(c) with that of Fig. 7 found in Ref. 2 indicates that the first function is wider and extends to even larger distances than the function in Ref. 2. The characteristics of the radial distribution function obtained herein for amorphous iron are certainly indicative of a highly disordered structure, a disorder that is also the cause of the very weak EXAFS signal observed herein. The amorphous iron studied herein shows a local structure, which is even more disordered than that shown[2] by the amorphous iron thin films and is well described by an asymmetric radial distribution function.

The assignment of a peak in the earlier neutron-diffraction studies[9,11] to oxygen neighbors of iron at 1.93 or 2.06 Å in an iron-oxide impurity drew our attention to the shoulder observed at ca. 1.6 Å in the Fourier transform shown in Fig. 6(b), a shoulder that could not be reproduced by introducing iron near neighbors at any reasonable distance. Hence we assumed, in agreement with both the neutron-diffraction analysis and the weak absorptions present at ca. -8 and $+7$ mm/s in the 78 K Mössbauer spectrum shown in Fig. 1, that the sample contains a small amount of iron-oxide impurity. Consequently, a second shell, see Table II, is assigned to oxygen neighbors of iron in the impurity. The absence of a model compound for this impurity yields a low precision for the parameters of the fit carried out with a symmetric Gaussian distribution. In spite of various attempts and in the absence of a Fe-O model compound, the fit of this shoulder could not be improved further than is shown in Fig. 6(b). The distance of 1.99 Å is reasonable in comparison with the values of 1.93 or 2.06 Å found[9,11] by neutron-diffraction measurements.

The peak at ca. 4.4 Å in the Fourier transform for amorphous iron in Fig. 5 seems to be related to some subsisting long-range order, an order that is similar to that found in

α-iron at a distance of ca. 4.7 to 4.9 Å. This observation is consistent with the results of the multiple-scattering calculations mentioned in Sec. III B.

In conclusion, the EXAFS results for amorphous iron may be analyzed with an asymmetric radial distribution function that is consistent with both earlier neutron-diffraction results[9,11] on bulk amorphous iron and earlier EXAFS results[2] on amorphous-iron thin films. Further, these results indicate a reduced average coordination number and a reduced minimum iron-iron distance, reductions that agree with the changes in the Mössbauer spectral hyperfine parameters.

ACKNOWLEDGMENTS

The authors appreciate the help of Professor A. Michalowicz, University of Paris 12, Créteil, and Dr. A. Hautot, University of Liège, in analyzing the EXAFS data. Further, the authors acknowledge, with thanks, the support obtained from the Ministère de la Communauté Française de Belgique for A.R.C. Grant No. 94/99-175, from the Fonds National de la Recherche Scientifique, Belgium, and from the Division of Materials Research of the U.S. National Science Foundation for Grant No. DMR-9521739.

[1] T. Egami, Rep. Prog. Phys. **47**, 1601 (1984).
[2] D. Chanderis, H. Magnan, G. Jezequel, K. Hricovini, G. Rossi, B. Villette, and J. Lecante, Phys. Scr. **T31**, 239 (1990).
[3] K. S. Suslick, D. A. Hammerton, and R. E. Cline, Jr., J. Am. Chem. Soc. **108**, 5641 (1984).
[4] K. S. Suslick, Sci. Am. **260**, 62 (1989); Science **247**, 1439 (1990).
[5] K. S. Suslick, T. Hyeon, and M. Fang, Chem. Mater. **8**, 2172 (1996).
[6] M. W. Grinstaff, A. A. Cichowlas, S.-B. Choe, and K. S. Suslick, Ultrasonics **30**, 168 (1992).
[7] W. C. Moss, D. B. Clarke, and D. A. Young, Science **276**, 1398 (1997); see also L. A. Crum and T. J. Matula, *ibid.* **276**, 1348 (1997).
[8] K. S. Suslick, S.-B. Choe, A. A. Cichowlas, and M. W. Grinstaff, Nature (London) **353**, 414 (1991).
[9] R. Bellissent, G. Galli, T. Hyeon, S. Magazu, D. Majolino, P. Migliardo, and K. S. Suslick, Phys. Scr. **57**, 79 (1995).
[10] M. W. Grinstaff, M. B. Salamon, and K. S. Suslick, Phys. Rev. B **48**, 269 (1993).
[11] R. Bellissent, G. Galli, M. W. Grinstaff, P. Migliardo, and K. S. Suslick, Phys. Rev. B **48**, 15 797 (1993).
[12] Y. Koltypin, G. Katabi, X. Cao, R. Prozorov, and A. Gedanken, J. Non-Cryst. Solids **201**, 159 (1996).
[13] K. V. P. M. Shafi, A. Gedanken, R. B. Goldfarb, and I. Felner, J. Appl. Phys. **81**, 6901 (1997).
[14] O. Rozenfeld, Y. Koltypin, H. Bamnolker, S. Margel, and A. Gedanken, Langmuir **10**, 3919 (1994).
[15] X. Cao, Y. Koltypin, G. Kataby, R. Prozorov, and A. Gedanken, J. Mater. Res. **10**, 2952 (1995).
[16] Q. A. Pankhurst, in *Mössbauer Spectroscopy Applied to Magnetism and Materials Science*, edited by G. J. Long and F. Grandjean (Plenum, New York, 1996), Vol. 2, p. 59.
[17] M. Eibschütz, M. E. Lines, and H. S. Chen, Phys. Rev. B **28**, 425 (1983).
[18] U. Gonser, M. Ackerman, H. J. Bauer, N. Blaes, S. M. Fries, R. Gaa, and H. G. Wagner, in *Industrial Applications of the Mössbauer Effect*, edited by G. J. Long and J. G. Stevens (Plenum, New York, 1986), p. 25.
[19] G. Longworth, in *Mössbauer Spectroscopy Applied to Inorganic Chemistry*, edited by G. J. Long (Plenum, New York, 1987), Vol. 2, p. 289.
[20] C. L. Chien, D. Musser, E. M. Gyorgy, R. C. Sherwood, H. S. Chen, F. E. Luborsky, and J. L. Walter, Phys. Rev. B **20**, 283 (1979).
[21] C. L. Chien, D. Musser, F. E. Luborsky, and J. L. Walter, J. Phys. F **8**, 283 (1978).
[22] J. Z. Jiang, J. Magn. Magn. Mater. **154**, 375 (1996).
[23] M. Liebs and M. Fähnle, Phys. Rev. B **53**, 14 012 (1996).
[24] R. D. Ernst, D. R. Wilson, and R. H. Herber, J. Am. Chem. Soc. **106**, 1646 (1984).
[25] B. Kolk, in *Dynamic Properties of Solids*, edited by G. K. Horton and A. A. Maradudin (North-Holland, Amsterdam, 1984), Vol. 5, p. 5.
[26] S. J. Campbell and H. Gleiter, in *Mössbauer Spectroscopy Applied to Magnetism and Materials Science*, edited by G. J. Long and F. Grandjean (Plenum, New York, 1993), Vol. 1, p. 241.
[27] U. Herr, J. Jing, R. Birringer, U. Gonser, and H. Gleiter, Appl. Phys. Lett. **50**, 472 (1987).
[28] Q. A. Pankhurst (unpublished).
[29] L. A. Grunes, Phys. Rev. B **27**, 2111 (1983).
[30] A. Di Cicco, M. Berrettoni, S. Stizza, E. Bonetti, and G. Cocco, Phys. Rev. B **50**, 12 386 (1994).
[31] J. E. Müller, O. Jepsen, and J. W. Wilkins, Solid State Commun. **42**, 365 (1982).
[32] T. A. Tyson, K. O. Hodgson, C. R. Natoli, and M. Benfatto, Phys. Rev. B **46**, 5997 (1992).
[33] D. S. Yang and G. Bunker, Phys. Rev. B **54**, 3169 (1996).
[34] V. G. Harris, S. A. Oliver, J. D. Ayers, B. N. Das, and N. C. Koon, Appl. Phys. Lett. **68**, 2073 (1996).
[35] E. Prouzet, A. Michalowicz, and N. Allali, J. Phys. IV **7**, C2-261 (1997).